Lowland Technology International 2016; 18 (3): 183-196
International Association of Lowland Technology (IALT): ISSN 1344-9656

Research Paper

Georisks during road tunneling in weathered quartz sand rock with faults under high-head of groundwater

B. Yuan [1], Y.S. Xu [2], S.L. Shen [3] and T. Hino [4]

ARTICLE INFORMATION

Article history:

Received: 19 May, 2016
Received in revised form: 15 July, 2016
Accepted: 20 July, 2016
Publish on: 28 December, 2016

Keywords:

Engineering geology
Fractured rock
Fissure water
Mining tunneling
Faulted fracture
Geo-hazard

ABSTRACT

This paper presents an investigation of georisks during mining tunnel construction in weathered quartz sand rock with faults at Fuyang, which is located at the southwest of Hangzhou, Zhejiang Province, China. Fuyang is a hilly region, where volcanic and intrusive rock masses are irregularly distributed, with the extensive development of fault zones and joint fractures. The Park Road Tunnels in Fuyang City will pass through the mountain in the city center and will be excavated in the lightly to weakly weathered quartz sand rock. The rocks are mainly crushable and are affected by fault zones and joint fractures. The fault zones and joints have large cavities filled with loose fragments and rich of fissure water. The rocks are classified into three grades based on the design code for road tunnels in China. The strength of the rock gradually decreases under the softening effect of abundant fissure water during construction. It was found that water ingress occurred at the entrance and the exit of the tunnel, the faults, and the contact zone between the hard and soft rock. Landslides had also occurred at the entrance and the exit of the tunnel in this case study.

1. Introduction

With the recent economic boom and urbanization in China, a large amount of infrastructure has been constructed not only in metropolitan cities but also in medium to small cities (Shi et al., 2013; Xiao et al., 2014; Iamtrakual et al., 2014). This infrastructure includes city roads (Sowmiya et al., 2015), highways, communication links, and transportation tunnels (Shen et al., 2015a, 2015b). The geological conditions include not only soft Quaternary deposits in Jiangsu (Du et al., 2014), Shanghai (Shen et al., 2013a, 2013b, 2014; Wu et al., 2015a; Dong et al., 2014; Tan et al., 2015a,b, 2016), Hangzhou (Wu et al., 2015b, 2015c), and Tianjin (Shen et al., 2014) but also various rocky conditions such as those found in Guangzhou (Cui et al., 2015a, 2015b), Shenzhen (Cui et al., 2016), and Chongqing. The construction methods used include open-cut excavation (Peng et al., 2011; Shen and Xu, 2011; Tan et al., 2015a, b, 2016), shield tunneling (Liao et al., 2009; Shen et al., 2010, 2014; Wu et al., 2015), and mining tunneling (Horpibulsuk et al., 2014; Shen et al., 2016).

[1] Research Associate, State Key Laboratory of Ocean Engineering, and Department of Civil Engineering, Shanghai Jiao Tong University, CHINA, taiyangdangkongzhao@sjtu.edu.cn
[2] Associate Professor, Collaborative Innovation Center for Advanced Ship and Deep-Sea Exploration (CISSE), Department of Civil Engineering, Shanghai Jiao Tong University, CHINA
[3] Professor & IALT member, State Key Laboratory of Ocean Engineering and Collaborative Innovation Center for Advanced Ship and Deep-Sea Exploration (CISSE), Department of Civil Engineering and Shanghai Jiao Tong University, CHINA, slshen@sjtu.edu.cn
[4] Guest Professor, Department of Civil Engineering, Shanghai Jiao Tong University, China and Professor, Institute of Lowland and Marine Research, Saga University, JAPAN, hino@ilt.saga-u.ac.jp
Note: Discussion on this paper is open until June 2017

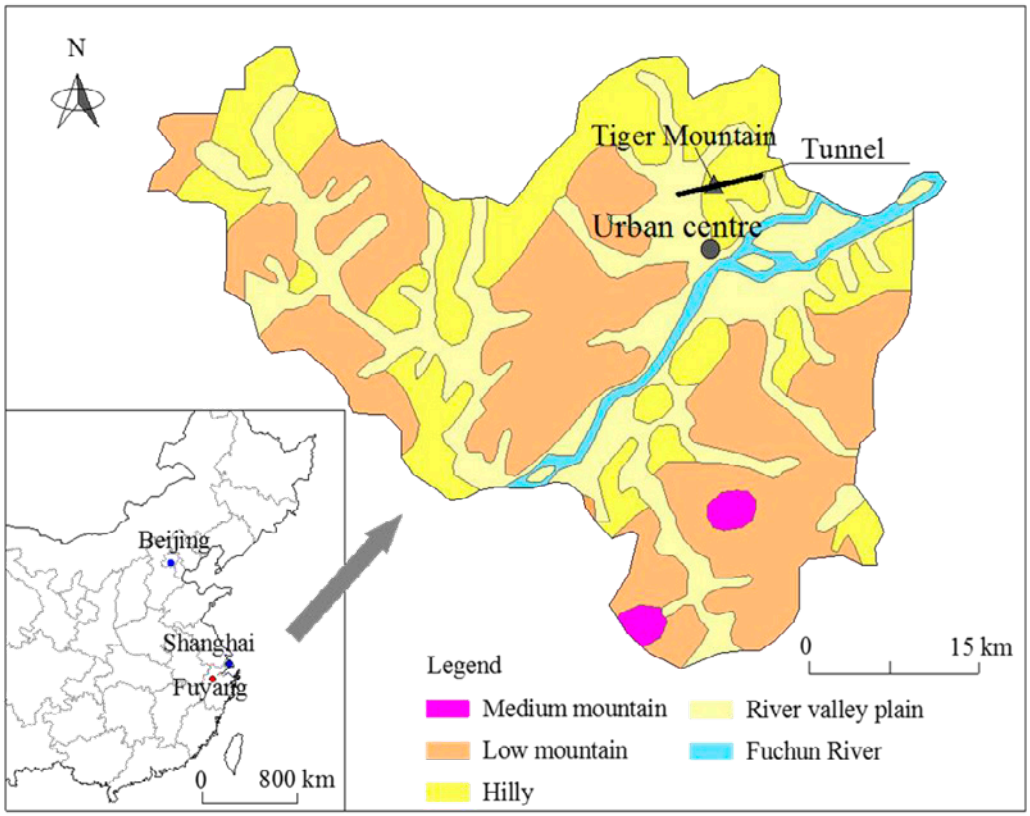

Fig. 1. Geomorphological map of Fuyang City, Zhejiang Province, China.

Infrastructure projects are often going through mountains and valleys in the mountain region due to the topographic features. Rock tunnelling has become prevalent in recent years for its superiority on shortening the length of the road and increasing the operation benefit (Tseng et al., 2001). Tunnelling is often associated with groundwater ingress from geological features such as faults zone and open fractures under high-head of groundwater (Tseng et al., 2001; Shahriar et al., 2008). Groundwater has impacts both in the construction stage and operation stage. The surrounding rock is easily destroyed from the weathering and the development of faults and joint fractures once excavation. After excavation, the stress state of disturbed zone of surrounding rock is changed resulting in the deformation of the rock, which will induce the expanding of the joint fracture. The consequent water ingress is developed (Shrestha et al., 2014; Zarei et al., 2011). Sometimes, groundwater will be contaminated by the recharge measurement or the tunnel construction (Day et al., 2004). The water ingress may result in the variation of PH value and content of metallic element such as Fe, Cu, Pb, and Zn in groundwater (Du et al., 2015a, b, 2016). The stability of tunnel structure gradually decreased due to the interaction of groundwater and lining. The strength of lining is lowered under the softening action of groundwater and the cracks of lining is generated under high water pressure as one of the channel of groundwater leakage in the operation stage. The long-term leakage of the groundwater in the operation will erode the lining and result in the ponding of tunnel (Shrestha et al., 2014; Tseng et al., 2001; Carranza-Torres et al., 2009).

Fuyang City, with an area 1831.2 km^2, is located in the north of Zhejiang Province, China, which is made up of hilly areas (75.7%), valley plains (21.6%) and water areas (2.7%) (Qian et al., 2008). The land area of Fuyang is dominated by hilly regions and is divided into two parts by the Fuchun River, forming an area with higher topography in the southeast with an elevation of 500 m to 1000 m, and a flatter topography in the northwest, as shown in **Fig. 1**. The water areas, including the Fuchun River and other rivers and streams of this region, recharge the aquifers by discharging water through the river or stream bed, thereby providing an abundant groundwater source (Qian et al. 2008). The strata in Fuyang are complex and are of a geological age ranging from the Middle Paleoproterozoic to the Quaternary.

The Park Road highway tunnels in Fuyang are planned to pass through Tiger Mountain which has an elevation of 388.2 m. The bedrock of the mountain is crushed and is affected by the faults which have developed at this site. In this study, faults are mainly extensional with large cavities filled with loose rock

fragments and abundant groundwater. Joint fractures in the rock mass are formed by the process of weathering and diastrophism. Both the faults and joints act as channels for water transmission and storage. The groundwater level in the site has a high elevation of 200 m locally. Under the high groundwater level, high water pressure is generated which acts on the rock mass after tunnel excavation (Song et al., 2015). This kind of geological and hydrological conditions present potential geo-hazards during tunnel construction, such as collapse, water ingress, landslide, and deformation of the bedrock.

The objective of this paper is to evaluate the potential risks to the construction of the Park Road tunnels in Fuyang City. First, the regional geology of Fuyang is introduced. Then the engineering geology and hydrogeology is investigated and an engineering geology assessment is conducted. To analysis the stability of the engineering, the classification of the rock mass is carried out (Rahmati et al. 2014). Finally, the potential geo-hazards during the construction of tunnels are discussed and corresponding preventative measures are proposed.

2. Geological formations around Fuyang

The ages of the strata in Fuyang City vary from the Middle Proterozoic to the Quaternary, with the Paleozoic and Jurassic volcanic rock masses being widely distributed. Intrusive rock represents 75.16 km^2 of the total area of outcrops found in the city, which includes Yanshanian intrusive rocks which are mainly distributed in Huyuan Town and the south of Xukou Town, while Jinningian intrusive rocks are distributed in the south of Changlv town. The lithological characteristics of the strata in Fuyang are complex, and the strata include granite-porphyry, quartz-orthophyre, granodiorite-porphyry, allgovite, moyite, and rhyolite porphyry and quartz felsophyre, as shown in **Fig. 2**. Foliations and joint fractures have developed in the rock masses under the action of gravity, and in places the joints occur densely and the rock masses are crushed (Qian et al., 2008).

Figure 2 also shows that several faults have developed in Fuyang city. These can be generally classified into four types, according to the fault trend: faults with a northeast (NE) trend, a northwest (NW) trend, a northeast-east (NEE) trend, and a northwest-west (NWW) trend. The NE faults are generally large scale with a width of tens to hundreds of meters and a length of up to tens of kilometers, they are extensional, and silication has occurred. The faults generally strike NE at an angle of 40° to 60°, and at an inclination of 70° to 90°. The NW faults are generally small scale and shorter in length. The faults strike NW at an angle of 320° to 335°, and the inclination angle ranges from 80° to 90°. The NEE faults are small scale, short in length, and less widespread. The faults strike NEE at an angle of 70° to 80° and the inclination angle ranges from 75° to 90°. The NWW faults are found in the south of Fuyang City, and occur at widths of about 20 m to 40 m, with lengths ranging from 2 km to 4 km, and inclination angles ranging from 80° to 90°. The rocks in the faults are completely crushed and silication is evident (Qian et al., 2008).

The Xiaoshan-Qiuchuan fault, the Kaihua-Anchun fault, and the Changhua-Putuo fault are the three main faults considered in this study. The Xiaoshan-Qiuchuan fault is located in the southwest of Fuyang city, the Kaihua-Anchun fault is located in the northwest, and the Changhua-Putuo fault is located in the north. The Xiaoshan-Qiuchuan fault is the largest of the three faults. It passes through the middle of Fuyang city and divides Fuyang into the northern tectonic region and the southern tectonic region. The proposed tunnels are located in the northern tectonic region.

3. Park Road highway tunnel

3.1 Engineering geology

The proposed Park Road highway tunnels are located in the northeast of Fuyang, starting at North Bridge Road and ending at Golf Road with a total length of 3.154 km. The highway tunnels are designed as two separate tunnels, the north tunnel and south tunnel, each having a maximum width of 13.5 m. The tunnels are planned to pass through Tiger Mountain, which has an elevation of 388.2 m and a natural slope ranging from 20° to 30°. The mountain above the tunnel entrance is flat in the lower part and steep in the upper part, with a slope height of 180 m and a slope angle of 20° to 30°. The entrance to the north tunnel is located in the side of the Tiger Mountain at a height of 10 m and a slope angle of 25° to 35°. The entrance to the south tunnel lies in flat ground. The exits of the north and south tunnels are situated in the mountain slope which has a height of 160 m and a slope angle of 25° to 45°. **Figure 3** shows the outline of the project, the location of the boreholes and faults.

In this study, the major strata present are the loose eluvial layer from the Quaternary Era, sandstone of the Upper Silurian series, and granodiorite from the third phrase of the Yanshanian period in the Pre-Quaternary Era. The distribution of rock strata in the south and north tunnels is shown in **Fig. 4**. The details of the strata from top to bottom are described as follows:

1) Loose eluvial layer of the Quaternary Era: This stratum mainly has mixed soils containing cohesive soil

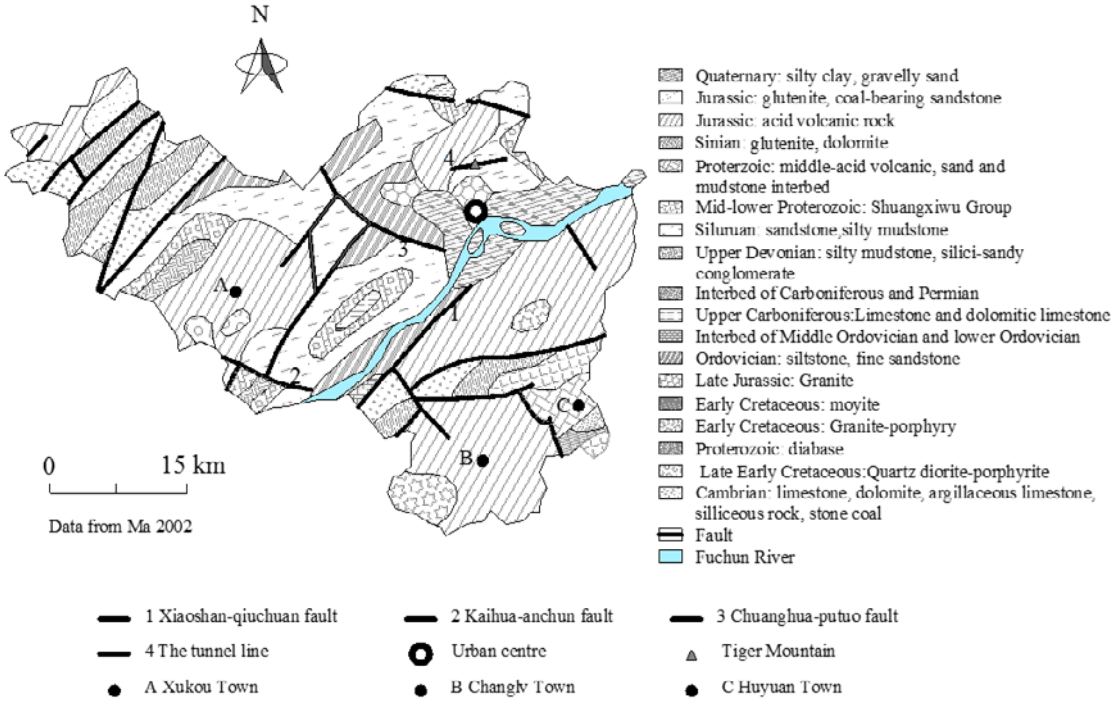

Fig. 2. Geological map of Fuyang City.

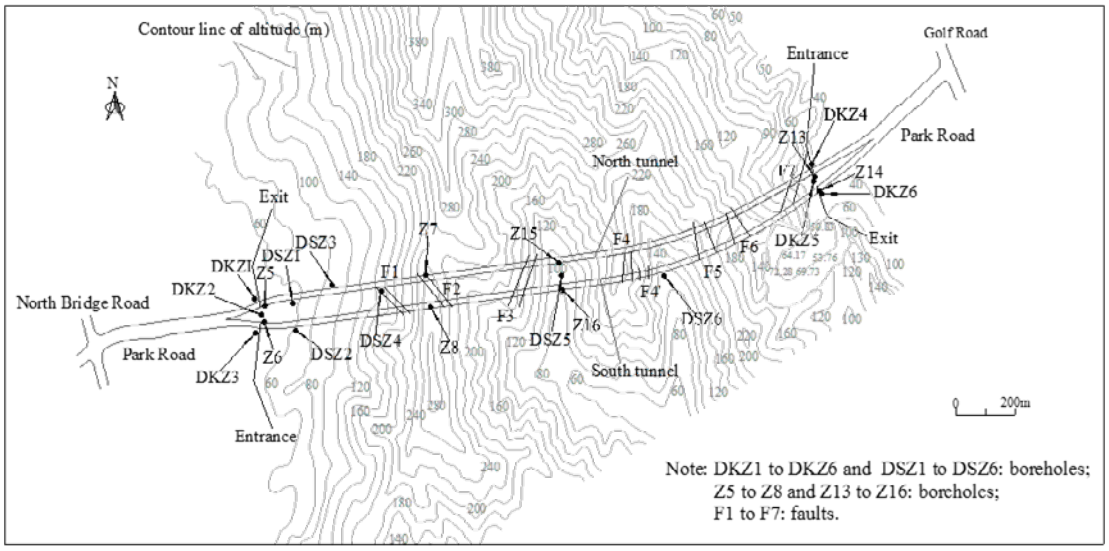

Fig. 3. Outline of the Park Road tunnel.

with a maximum thickness of about 15.0 m. The main rock within the mixed soils is mostly loose sandstone mixed with silty clay. The stratum is primarily distributed in a piedmont plain and hillside and is subdivided into four major layers:

(i) Miscellaneous fill (labelled in **Fig. 5** as 1-1): This layer consists of mainly silty clay with construction waste. This layer is distributed locally with a thickness of 0.30 to 4.20 m.

(ii) Plain fill (labelled 1-2): This layer is grey-yellow fill in an uncompact state, and consists mainly of crushed stone and silty clay containing gravel, and some plant roots. The crushed stone are weathered rock with the content about 28%. The layer is distributed throughout the study area with a thickness of 0.30 to 8.40 m.

(iii) Silty clay with gravel (labelled 2): This layer is grey-brown and grey-yellow soil in a hard and plastic state, and consists of mainly silty clay and about 20 to 30% secondary gravelly sand. The layer was only found in some of the boreholes located in the subgrade layer which has a thickness of 1.20 to 5.90 m.

(iv) Silty clay (labelled 3): This layer is grey and grey-black soil in a saturated and soft plastic state, and consists mainly of silty clay with a small amount of humus,

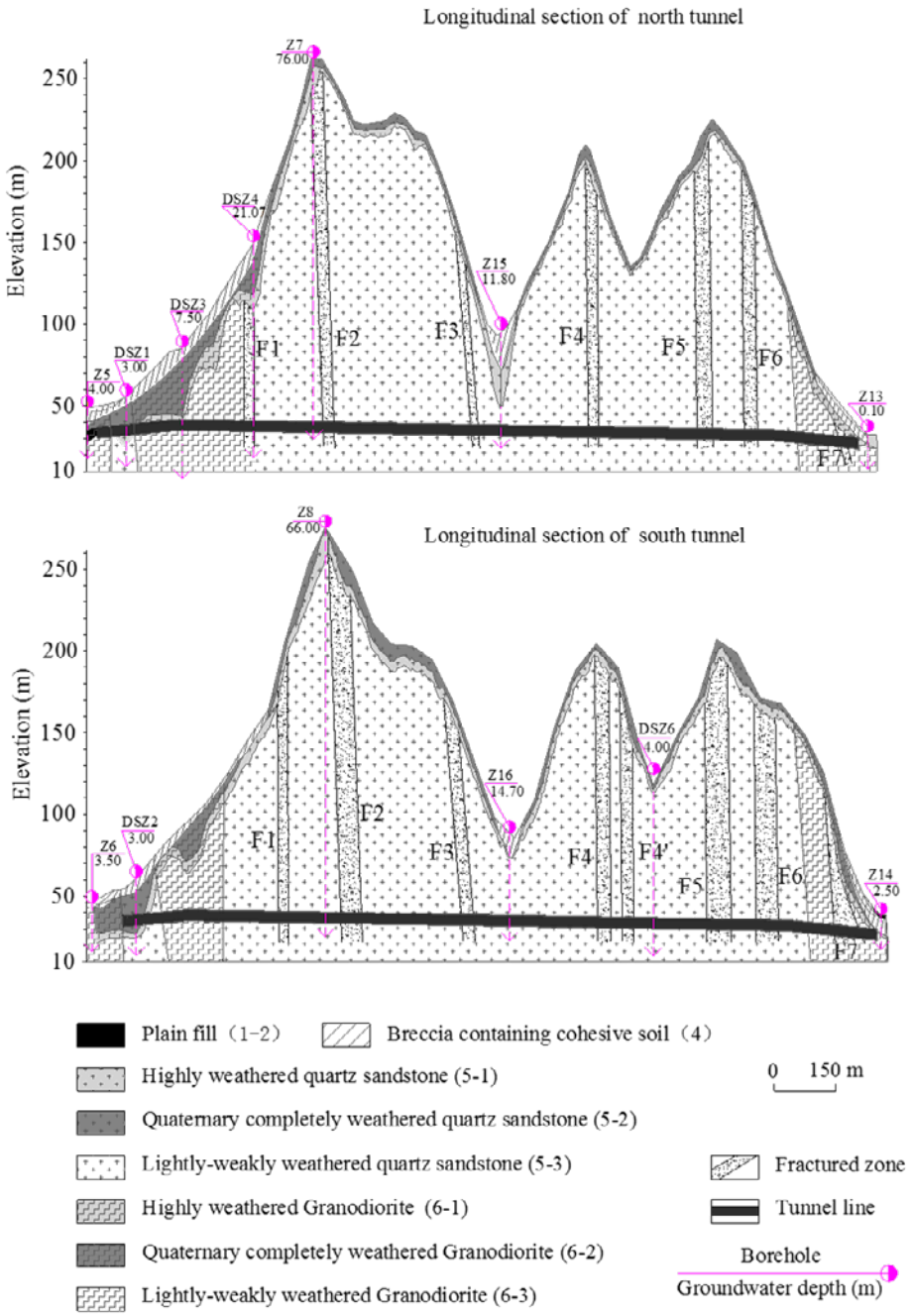

Fig. 4. Geological profiles of the tunnels.

and partly flowing plastic mucky clay. This layer was only found in some of the boreholes located in the subgrade layer with a thickness of 0.50 to 3.40 m.

(v) Gravel with clay (labelled 4): this layer is grey-yellow and yellow-brown soil in a dense and partially medium dense state. The soil mainly consists of 35% crushed stone with a particle diameter of 20 to 60 mm, 25% gravel with a particle diameter of 2 to 20 mm, and 30% sand; with clay and partially weathered granite. The layer occurs throughout the field site at a thickness of 1.4 to 14.10 m. The geological properties of the soil layers are described in **Fig. 5**.

2) Sandstone of the Upper Silurian Period in the Pre-Quaternary Era: This stratum is grey and cyan-grey sandstone interbedded with siltstone and shale. Based on the degree of weathering as shown in **Table 1** (MOHURD, 2014), the layer is divided into three sub-layers as follows:

(i) Completely weathered quartz sandstone (labelled in **Fig. 6** as 5-1): this layer is cyan-grey and cyan

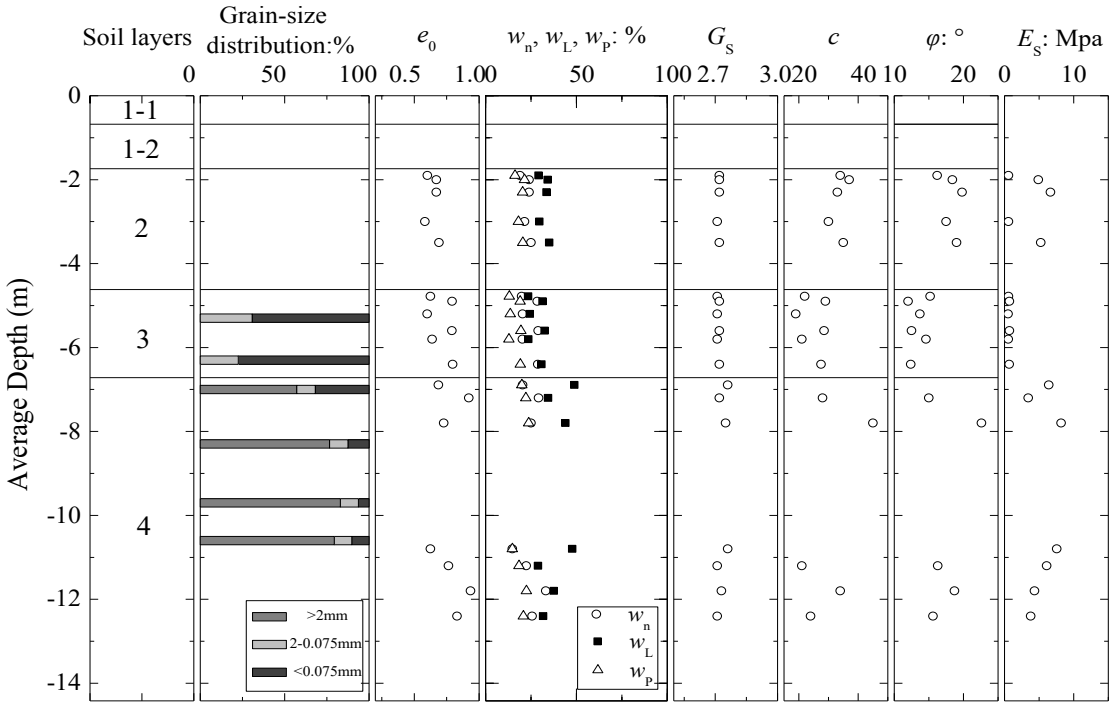

Note: w_n is natural water content; w_L is liquid limit; w_P is plastic limit; e_0 is void ratio; G_S is specific gravity; c is cohesion; φ is internal friction angle; E_S is compression modulus.

Fig. 5. Geotechnical properties of the soil layers.

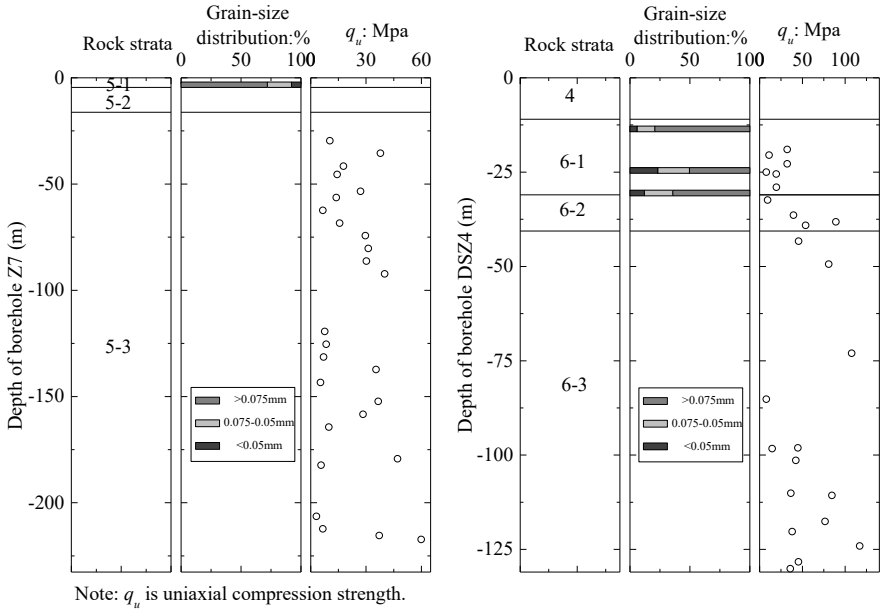

Note: q_u is uniaxial compression strength.

Fig. 6. Geotechnical properties of the rock strata.

completely weathered quartz sandstone with a thickness of 3.0 to 27.20 m. The structure of the rock mass has been destroyed and the rock core is in the form of sand. Joint fractures have developed in the rock mass and are filled with mainly siliceous materials and secondary hydromica. The rock core mass fragments when cut.

(ii) Highly weathered quartz sandstone (labelled 5-2): this layer is cyan-grey and cyan highly weathered quartz sandstone with a thickness of 0.8 to 34.2 m. The structure of the rock mass has mostly been destroyed and the rock core is crushed stone and sand. The joint fractures developed in the rock mass are filled with mainly siliceous materials and secondary hydromica. The rock core mass presents as chunks and short columns when cut.

Table 1. Classification of degree of weathering (Dearman et al., 1978; MOHURD, 2014).

Weathering degree	Characteristics
Unweathered	Structure and texture stay unchanged; fresh rock.
Lightly weathered	Structure, texture and color of mineral stay unchanged basically; partial fissure surface is rendered by iron and manganese or discolored slightly.
Moderately weathered	Structure and texture are partially destroyed; mineral color changes greatly; fissure surface weathered more severely.
Highly weathered	Structure and texture are mostly destroyed; mineral color changes greatly; alteration and weathering occur in feldspar, mica and magnoferrite.
Completely weathered	Structure and texture are completely destroyed and disintegrated into earth and sand; mineral color changes completely without lustre; minerals are weathered into secondary minerals except quartz.

(iii) Lightly-weakly weathered quartz sandstone (labelled 5-3): this layer is cyan-grey and cyan lightly-weakly weathered quartz sandstone, which mainly consists of sand and secondary interstitial matter. The rock mass is in the form of sand. The sand is mainly quartz and secondary feldspar and rock debris. The interstitial material is mostly siliceous materials and secondary hydromica. The rock mass has basal cementation, with good sorting, the fracture structure is apparent, and the cracks in the rock mass are filled with sericite. The rock core is crushed stone and sand. The integrity of the rock ranges from fragmented to complete. This layer is distributed within the main body of the tunnels.

3) Granodiorite in the third phrase of the Yanshanian Period: This stratum is granodiorite with a hypidiomorphic granular shape which mainly consists of feldspar secondary quartz, and a slightly dark mineral. According to the degree of weathering as shown in **Table 1** (MOHURD, 2014), this layer is classified into three sub-layers as follows:

(i) Completely weathered granodiorite (labelled in Fig. 6 as 6-1). This layer is a light grey completely weathered granodiorote in a dense and medium dense state. The shape of the rock mass is destroyed and has been weathered into chunks of sand which can be easily crumbed. The bottom of this sub layer contains more blocks of rock. This layer is distributed in the entrance and the exit of the tunnels with a thickness of 1.90 to 35.10 m.

(ii) Highly weathered granodiorite (labelled 6-2). This layer is shallow with green highly weathered granodiorite, with fracture development. The structure of this layer has been mostly destroyed. The core of the rock mass is in chunks and partially stumpy when cut. The thickness of the layer ranges from 1.20 to 9.60 m.

(iii) Lightly-weakly weathered granodiorite (labelled 6-3). This layer is shallow with grey-green lightly-weakly weathered granodiorite with a hypidiomorphic granular structure, which consists mainly of feldspar, secondary quartz, and a slightly dark mineral. The rock has a hypidiomorphic granular structure with a high hardness. The integrity of the rock is complete and part of the rock has a cataclastic structure and carbonatation has occurred. **Figure 6** shows the geological properties of the rock strata.

3.2 Tectonics

Affected by tectonic movement, joint fractures have extensively developed in the granodiorite and the quartz sandstone surrounding the tunnel. The degree of bonding between layers is medium-low. The integrity of the rock mass ranges from complete to crushed, while the rock mass in the fault fracture zones is crushed. The saturated compressive strength of the bed rock is high and that of the lightly-weakly weathered rock is medium. Therefore, the bed rock can be classified as a hard rock with a high mechanical strength. Joints and several faults are largely distributed in the weathered rock mass in this study.

3.2.1 Faults

The Xiaoshan-Qiuchuan fault zone in Fuyang involves a series of parallel faults with a total width of 1000 m (Zhang et al., 2008). This fault is mostly overthrust. The Xiaoshan-Qiuchuan deep faults formed in the late Proterozoic, and the formation of the Xiaoshan-Qiuchuan fault in different locations and different periods are obviously different (Yao et al., 2008). In the late Jurassic Period, the movement of the Xiaoshan-Qiuchuan fault is mainly overthrust, meaning that the Tangjiawu and the Kangshan groups are placed in the Jurassic Huangjian group, developed under compression. Since the Early Cretaceous, tectonic movement has forced this group into tension, which has contributed to the formation of the Yanshanian fault and rift basin and to the sedimentary strata of the Cretaceous group. The fault has directly controlled the sedimentary strata since the Paleozoic, thus it has developed completely different strata and geomorphic units. The most active movement is indicated by the appearance of compressional thrust and tension rift in succession (Zhang et al., 2008). The general trend of the Xiaoshan-Qiuchuan fault is about 50° and the orientation is northwest with a dip of 65°. Extended by the major Xiaoshan-Qiuchuan fault zone, seven faulted fractures have developed in the excavation

Table 2. Attitudes of fault fracture zone.

Fault	Strike (°)	Dip angle (°)	Inclination
F1	N42°W	82°	SW
F2	N39°W	85°	SW
F3	N35°E	72°	SE
F4	N10°E	84°	SE
F5	N31°W	81°	SW
F6	N51°W	79°	SW
F7	N55°W	82°	SE

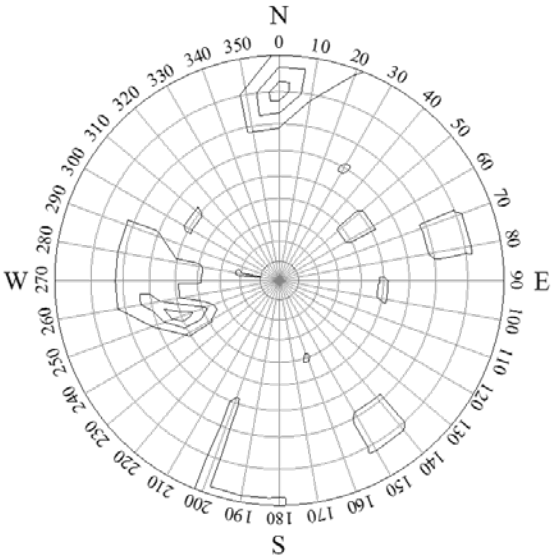

Fig. 7. Pole diagram of joints.

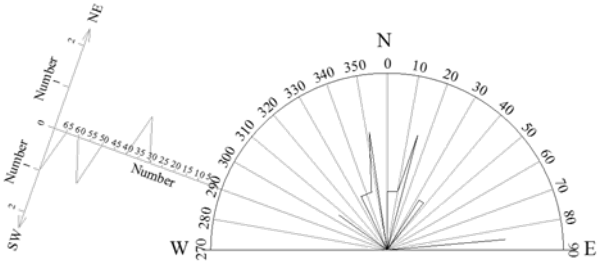

Fig. 8. Rose diagram of joints.

area. The locations of the fault fracture zones are presented in **Fig. 3** and the attitudes observed in **Table 2**.

3.2.2 Joint fractures

Joint fractures are the weak structural planes of the rock mass, and they have a greater effect than the main rock on the deformation of rock mechanical properties, strength, failure modes and failure mechanisms (Gupta et al. 1999). For instance, the degree of development of the joint fractures affects the rock engineering properties significantly. The physical and mechanical properties are different between unfractured rock and rock with joint fractures. The shear strength and tensile strength of the rock mass are significantly reduced by the presence of joint fractures and the integrity of the rock mass can be easily destroyed under the simultaneous action of shear and tension (Huang et al., 2013). Furthermore, joint fractures are considered to be important channels for groundwater flow (Zarei et al., 2011).

The characteristics of 35 sets of joint fractures, including orientation, infilling and arrangement of the joint fractures, were investigated at the site before construction. **Figure 7** shows a pole diagram of the joint fractures. The radial lines in the figure represent the inclination of the joint fracture which varies from 0° to 90°, and the concentric circles illustrate the dip angle. **Figure 8** shows a rose diagram of the joint fractures. The angle indicated by the radial lines shows the average inclination of the joint set, and its length expresses the number of the joint set. The general tendency of the joint fractures is in the direction of north and west. Four sets of joint fractures presented in **Table 3** influence the stability of the rock mass surrounding the tunnel. The four sets affecting the rock around the tunnel strike west and have less dip. They are shear joints, which are mainly parallel to the tunnel orientation and partially intersect the tunnel at an acute angle.

3.3 Hydrogeology

The groundwater in the exploration area can be divided into phreatic aquifer water and bedrock fissure water.

1) Phreatic aquifer water. Phreatic aquifer water is contained in the upper eluvial or diluvial Quaternary, which has pebbly silty clay. The aquifer effected by the climate change (Doan et al., 2015; Mustaffa et al., 2015) is distributed in the piedmont plain around the proposed tunnel, with a buried depth of less than 2.0 m in the rainy season and an abundant water volume. The phreatic aquifer is recharged by rainfall and surface runoff, which flows downward along the slope, discharges to the toe of the slope, and then connects with the shallow phreatic aquifer in the plain area (Doan et al., 2014). The buried depth of the phreatic aquifer is about 0.30 to 8.00 m. The level of groundwater varies from 0.50 to 1.50 m.

2) Bedrock fissure water. The bedrock fissure water is mainly stored in the upper Silurian litharenite. The fissure water is unevenly distributed due to the inhomogeneous development of a weathered fissure. The fissure water, which is recharged by rainfall, is abundant, and it flows along the slope, and discharges in the toe of the slope or along underground runoff.

Water pressure tests were conducted on the weathered bedrocks. The deduced Hydraulic conductivity of weathered granodiorite is 10-3 to 10-2 m/d with the characteristic of micro Hydraulic conductivity. Since the Hydraulic conductivity of weathered quartz sandstone was not obtained in this case, according to the related

engineering experience in this region, the empirical value of Hydraulic conductivity of weathered quartz sandstone is 10^{-3} to 10^{-2} m/d and the value of the strata of silty clay containing gravel is 0.0016 m/d (Mao et al., 2009). The confined water head in borehole DSZ5, whose location is shown in **Fig. 3**, is 5 m higher than the elevation of the mouth of the borehole which has a flow rate of 2 to 3 m^3/hour. The confined water head in borehole DSZ6 is 6 m higher than the elevation of the mouth of the borehole, which has a flow rate of 5 to 7 m^3/hour.

3.4 Evaluation of geological conditions

3.4.1 Classification of rocks

Rock mass classification is carried out, based on the code for design of road tunnels in China (CMCT, 2004). First, a preliminary classification is carried out based on the basic quality index of the rock mass by considering the degree of hardness and the integrity of the surrounding rock mass. The degree of hardness is qualitative and is evaluated based on the rock mass reaction under hammering and water immersion. The type of rock mass can be divided into hard rock, relatively hard rock, relatively soft rock, soft rock, and extremely soft rock. Uniaxial saturated compressive strength R_c is used to evaluate the degree of hardness of the rocks. The integrity is expressed by the integrity coefficient F_c, which is qualitative and is evaluated based on the characteristics of the rock structural planes, including the development degree, the binding degree of the major joint, and the type of major structural plane. The corresponding structural type of rock mass can be classified as: complete, relatively complete, relatively crushed, crushed, and extremely crushed. The basic quality index of rock mass, BQ, is determined based on the degree of hardness and the integrity of the rock mass, which can be calculated by an expression which combines R_c and F_c.

Detailed classification is then conducted based on an amended BQ ([BQ]) by considering some modifying factors. BQ should be modified in the following situations: 1) Groundwater is present; 2) Where the stability of the surrounding rock mass is affected by weak structural surfaces and is controlled by one particular surface; 3) There is high initial stress around the rock mass. [BQ] can be calculated by comprehensively considering the modified coefficients of groundwater, weak structural surface, and initial stress. The rock mass can be classified into six degrees, I, II, III, IV, V, and VI, according to the qualitative features of the surrounding rock mass and the value of [BQ] as shown in **Table 4**. Based on this approach, the surrounding rock mass of the mountain tunnel can be divided into three grades which are presented in **Fig. 9**.

4. Geo-hazards assessment

The geological formation at the study site is mostly faulted structural belts and weathered rock with joint development, causing difficult construction conditions. Ceiling collapse of the surrounding rocks, leakage and water spraying along the fault are likely to occur during the excavation. Based on the geological and hydrological conditions, the potential hazards of the case study are predicted and corresponding countermeasures are proposed.

4.1 Collapse

The potential hazards during the construction and operation of the tunnel according to the grades of the surrounding rock mass are presented as follows:

1) For grade III rock, the rock mass is stable. Blocks of rock may easily drop along the rock surface or small collapses may occur in the arches of the tunnels if a retaining and protective structure is not present. The side wall is basically stable. The rock mass is presented as a cataclastic structure, and the groundwater is bedrock fissure water. Drop leakage may occur during construction in the rainy season.

2) For grade IV rock, the bedrock is relatively crushed. Large collapses may happen in the arch without a proper retaining and protective structure. The side wall is basically stable. Also, the stability of the rock mass around the tunnel is poor due to the influence of the fracture zone (Shi et al., 2014). Groundwater in the fracture zone is relatively abundant. Some leakage may occur during the excavation.

3) For grade V rock, the bedrock is crushed. Large collapses may occur in the arch without a retaining and protective structure. The stability of the side wall is poor and small-medium collapses may occur. Medium deformation may occur in the soft fracture zone. Groundwater in the fracture zone is relatively abundant and leakage may arise during excavation. Furthermore, large water ingress and collapse may occur in the core of the fault zone.

4.2 Water ingress

Water ingress is a common geo-hazard during excavation in a rock mass with water-conducting faults which establish a hydraulic connection in a highly permeable stratum interbedded with a slightly permeable

Table 3. Attitudes of joint fractures.

Joint fractures	Strike (°)	Dip angle (°)	Inclination	Stretching degree	Surface feature	Infilling
J1	N79°W	35	SW	<1 mm	Parallel, smooth	None
J4	N72°W	42	SW	<1 mm	Parallel, smooth	Water
J7	N81°W	27	SW	<1 mm	Parallel, smooth	Less filling
J14	N72°E	31	SE	<1 mm	Intersect, smooth	Water, less filling

Table 4. Classification of rock mass around the road tunnel (CMCT, 2004).

Grade	Qualitative features	*BQ* or [*BQ*]
I	Hard rock, complete, large bonded or large thick-layered structure	>550
II	1. Hard rock, relatively complete, blocky or thick-layered structure; 2. Relatively hard rock, complete, blocky bonded structure	550-451
III	1. Hard rock, relatively crushed, blocky mosaic structure; 2. Relatively hard rock or relatively weak hard rock, relatively complete, blocky or medium thick-layered structure	450-351
IV	1. Hard rock, crushed, cataclastic structure; 2. Relatively hard rock, relatively crushed to crushed, mosaic cataclastic structure; 3. Relatively soft rock or interbedded layer of soft rock and hard rock with predominance of soft rock, relatively complete to relatively crushed, medium-thin -layered structure Soil : 1. Compacted or diagenetic cohesive soil and sandy soil; 2. Loess; 3. Calcareous and ferruginous cemented gravel soil, cobbly soil and large boulders	350-251
V	1. Relatively soft rock, crushed; 2. Soft rock, relatively crushed to crushed; 3. Extremely crushed rocks, broken, cracked, or loose structure Quaternary semi-hard to hard plastic cohesive soil, slightly wet gravel, cobbly, round gravel, dust, and loess. Non-cohesive soil is loose. Clay and loess is soft	≤250
VI	Soft plastic cohesive soil, wet saturated silty sand, or soft soil	

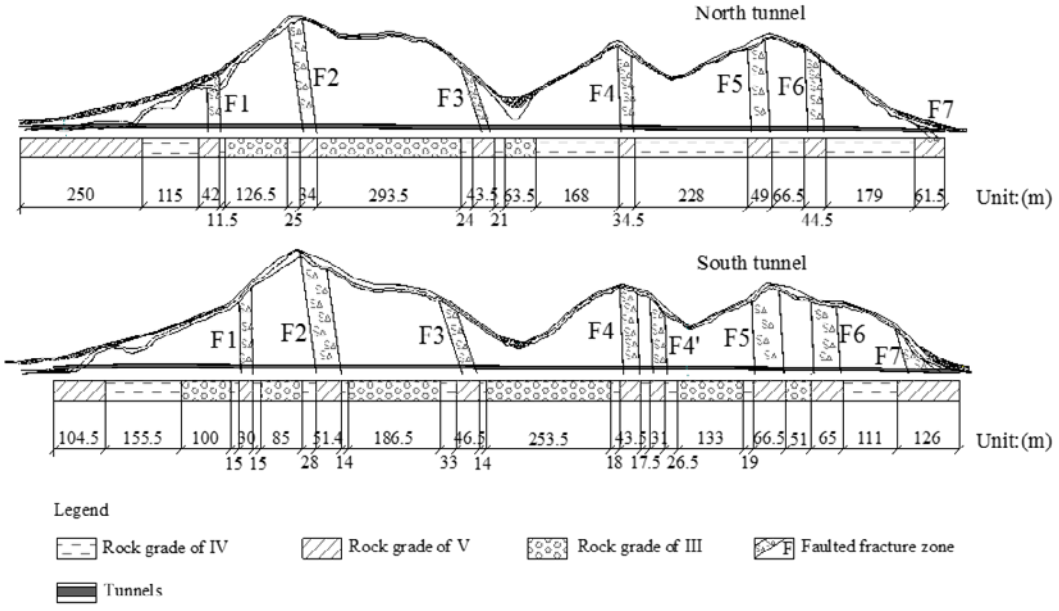

Fig. 9. Grade of the surrounding rock mass.

stratum. Water-bearing fissures are constantly expanding under high water pressure, and the impermeable rock mass is spilt, thus leading to water ingress (Li et al., 2015). The tunnel in the case study passes through the sedimentary stratum of the Upper Silurian where the tensional faults are highly developed and abundant fissure water is present. Water ingress may occur in some segments of the tunnel due to the complex geological conditions. Firstly, there may be a large water ingress at the entrance and the exit of the tunnel;

secondly, the places near faults such as F1, F2, and F3, have a greater risk of large water ingress because the fractured zone in a fault is rich in groundwater; thirdly, in the sedimentary stratum of the Upper Silurian developed in the interlayer fissure zone, large streams of water are probably produced during the excavation, especially in the two hills as shown in **Fig. 4**. In the pass area, the rock grade is IV and V and the rock is crushed. During drilling, there could be a gush of fissure water. Finally, in the tunnel site surrounded by intrusive rock, the leaking of groundwater is mainly by dripping and linear flow, with some spraying or small streams of water. Furthermore, a mass of water ingress is likely to occur in the contact zone of hard and soft rock. To mitigate against potential water ingress, water plugging is the main approach together with auxiliary drainage measures. Timely grouting and tunnel support should be implemented to reduce the risks to tunnel construction and operation (Zhao et al., 2013).

4.3 Landslide

When a tunnel passes through a mountain slope, landslides may occur, and these will induce deformation and cracking of the tunnel (Wu et al., 2012). In the study site, the entrance and exit of the tunnel are the likely locations for a possible landslide. The terrain at the site of the tunnel entrance slopes gently, at a height of about 10 to 20 m. Residual soil and highly and lightly weathered rocks are distributed in the upper section and to the sides of the tunnel entrance site, which reduce the slope stability after excavation. Support measures should be adopted. The lower sections of the tunnel are surrounded by moderately weathered rock with relatively good stability. However, crushed rock can partially block the exit from the rock mass and these can easily slide along the slope. Therefore, shotcreting and rock bolt support is necessary on the slope.

The terrain of the tunnel exit slopes relatively steeply. Residual soil and highly weathered rocks with poor stability are distributed in the upper section and to the sides of the tunnel exit. The overlying quaternary strata are medium dense and the content of cohesive soil contained in the fill is less dense. Without proper corresponding supporting and lining measures, landslide induced by the displacement of the soil may easily occur under the scouring action of heavy rain.

As the stability of the slope at the entrance and exit of the tunnel after excavation is poor, slope excavation is proposed. Appropriate slope ratios are suggested as 1:1.5 for the surface overlying Quaternary sediment, 1:0.75 for the surface overlying highly weathered rock, and 1:0.5 for the surface overlying lightly weathered rock. Also, the slope should be excavated in steps with a height of each step of less than 8 m. Intercepting dikes are proposed to be constructed at the top and on the surface of the slope. Support systems such as anchors, hanging nets, and shotcrete should be used for the unstable surfaces, based on practical experience.

4.4 Large deformation

Deformation of the surrounding rock mainly occurs when the rock stress is greater than the yield strength of plastic rock, which causes the surrounding rock to squeeze out along the space where there is low resistance. Large deformation has been a significant problem in road tunnel construction. Large deformations of the surrounding rock may damage the lining, which will result in delays in excavation. To evaluate the deformation of the bedrock, various factors including geological stress, specific properties of the rock, the softening mechanism caused by excavation, rock pressure and its strengthening effect should be considered (Wu et al., 2015d).

According to the geology of the site, the rock mass surrounding the tunnel is mainly quartz sandstone of a low rock grade. The preliminary determination of the large deformation of the surrounding rock is based on the stress ratio, R_0/R_c (where R_0 is rock stress and R_c is uniaxial compressive strength). When the ratio is higher than 4, a large deformation is easily produced. In this case study, the average value of R_c for the lightly weathered rock is 50 MPa, and for the slightly weathered or unweathered quartz sandstone, R_c is higher than 30 MPa. The rock stress is estimated as 10 to 20 MPa and the R_c is estimated to be higher than 18 MPa. Thus, the stress ratio is 0.6 to 1.0, which is less than 4, and therefore large deformation is not a risk. However, fault belts and joint fractures have developed at the site of the case study which is beneficial for the accumulation of groundwater. The strength of the surrounding rock decreases under the softening action of the groundwater, which causes plastic deformation. The mechanical properties of the surrounding rock will then decrease and deformation of the surrounding rock will occur due to the disturbance caused by the excavation.

5. Conclusions

This paper analyses the geo-risk for the Park Road tunnel in Fuyang City based on the geological and hydrogeological characteristics. An assessment of the engineering geology is conducted and the potential

hazards of the case study are predicted. The following conclusions can be drawn.

1) The geology in Fuyang City is complex due to the different eras forming the strata. Volcanic rock mass and intrusive rock mass are irregularly distributed in the city, with the development of deep faults and joint fractures, which are rich in bedrock fissure water.

2) The proposed road tunnel is to be excavated in the lightly to weakly weathered quartz sand rock. Joint fractures of weathered rock and several faults are distributed in the area. Four sets of the joint fractures influence the stability of the rock surrounding the tunnel. Seven extensive faults have developed in this region, and have the characteristics of poor cementation, good transmissibility, extended length and large width, providing good conditions for groundwater recharge. The main types of groundwater present are phreatic water and fissure water, with a high water pressure.

3) The rock at the site is graded as grade III with stability, grade IV which is relatively crushed, and grade V which is crushed, based on the design code for road tunnels in China. Without a proper retaining and protective structure during excavation, collapse and water leakage are likely to occur in the rock mass of grades IV and V.

4) Where there is development of faults with joints, the geo-hazards including water ingress, landslide, and deformation of surrounding rock, should be predicted before tunnel construction. Although large deformation of the surrounding rock is not a risk in this case study, the strength of the surrounding rock will decrease under the softening effect of the abundant groundwater, which will result in plastic deformation. Water ingress can easily occur at the entrance and exit of the tunnel, the faults, and the contact zone of hard rock and soft rock. Landslides are also likely to occur at the entrance and exit of the tunnel in this case study.

Acknowledgements

The research work described herein was funded by the National Basic Research Program of China (973 Program: 2015CB057806). These financial supports are gratefully acknowledged.

References

Carranza-Torres C, Zhao J., 2009. Analytical and numerical study of the effect of water pressure on the mechanical response of cylindrical lined tunnels in elastic and elasto-plastic porous media. Intl. J. Rock Mechanics and Mining Sciences, **46** (3): 531-547.

Chongqing Communication Research institute (CMCT), 2004. Vocational Standard of the P.R.C. Code for Design of Road Tunnel (JTGD70-2004). China communication press, Beijing: 73-75 (in Chinese).

Cui, Q.L., Shen, S.L., Xu, Y. S., Wu, H.N. and Yin, Z.Y., 2015a. Mitigation of geohazards during deep excavations in karst regions with caverns: a case study. Engineering Geology, **195**: 16-27.

Cui, Q.L., Wu, H.N., Shen, S.L., Xu, Y.S. and Ye, G.L., 2015b. Chinese karst geology and measures to prevent geohazards during shield tunneling in karst region with caves. Natural Hazards, **77** (1), 129-152.

Cui, Q.L, Wu, H.N., Shen, S.L. and Xu, Y.S., 2016. Geological difficulties and countermeasures for socket diaphragm walls in weathered granite in Shenzhen, China. Bulletin of Engineering Geology and the Environment, **75** (1): 263-273.

Day, M.J., 2004. Karstic problems in the construction of Milwaukee's Deep Tunnels. Environmental Geology, **45** (6): 859-863.

Dearman, W.R., Baynes, F.J. and Irfan, T.Y., 1978. Engineering grading of weathered granite. Engrg. Geol., **12**: 345-374.

Dong, Y.P., Burd, H., Houlsby, G. and Hou, Y.M., 2014. Advanced finite element analysis of a complex deep excavation case history in Shanghai. Front. Struct. Civ. Eng., **8** (1): 93–100.

Doan, Q.T., Don, N.C., Chen, Y.C. and Mishra, P.K., 2015. Applying numerical method to understand the effect of climate change on the salinity intrusion in Ca River Basion, Vietnam. Lowland Technology International, IALT, **17** (2): 93-104.

Doan, Q.T., Nguyen, C.D., Chen, Y.C. and Pawan, K.M., 2014. Modeling the influence of river flow and salinity intrusion in the Mekong River Estuary, Vietnam. Lowland Technology International, IALT, **16** (1): 14-25.

Du, Y.J., Jiang, N.J., Liu, S.Y., Jin, F., Singh, D.N., Puppala, A.J., 2014. Engineering properties and microstructural characteristics of cement-stabilized zinc-contaminated kaolin. Canadian Geotechnical Journal, **51** (3): 289-302.

Du, Y.J., Fan, R.D., Reddy, K.R., Liu, S.Y. and Yang, Y.L. 2015a. Impacts of presence of lead contamination in clayey soil-calcium bentonite cutoff wall backfills. Appl. Clay Sci., **108**: 111-122.

Du, Y.J., Fan, R.D., Liu, S.Y., Reddy, K.R. and Jin, F., 2015b. Workability, compressibility and hydraulic conductivity of zeolite-amended clayey soil/calcium-bentonite backfills for slurry-trench cutoff walls. Engrg. Geol., **195**: 258-268.

Du, Y.J., Yang, Y.L., Fan, R.D. and Wang, F., 2016. Effects of phosphate dispersants on the liquid limit, sediment volume and apparent viscosity of clayey soil/calcium-bentonite slurry wall backfills. KSCE J. Civ. Engrg., **20** (2): 670-678.

Gupta, A.S., Seshagiri, R.K., 1999. Weathering effects on the strength and deformational behaviour of crystalline rocks under uniaxial compression state. Engrg. Geol., **56** (2000): 257-274.

Horpibulsuk, S., Wijitchot, A., Nerimitknornburee, A. and Shen, S.L., 2014. Factors influencing unit weight and strength of lightweight cemented clay. Quarterly Journal of Engineering Geology & Hydrogeology, **47**: 101-109.

Huang, R.Q., Li, Y.R., Qu, K. and Wang, K., 2013. Engineering geological assessment for route selection of railway line in geologically active area: a case study in China. J. Mountain Sci., **10** (4): 495-508.

Li, T.B., Zuo, Q.K., Meng, L.B., and Xue, D.M., 2015. An approach on the types and mechanisms of water inrush in traffic tunnel constructions in China. Engineering Geology for Society and Territory, **6** (78): 449-452.

Liao, S.M., Liu, J.H., Wang, R.L. and Li, Z.M., 2009. Shield tunneling and environment protection in Shanghai soft ground. Tunneling and Underground Space Technology, **24** (4): 454–465.

Mao, C.X., Duan, X.B. and Mao Y.P., 2009. Dikes Engineering Manual. China Waterpower Press: 24-29 (in Chinese).

Ministry of Housing and Urban-Rural Development of the People's Republic of China (MOHURD), 2014. Standard for engineering classification of rock mass (GB/T50218-2014). China Planning Press: 8-9.

Mustaffa, A.A., Rasib, A.W., Razi, M.A.M., Adnan, M.S. and Tan, L.W., 2015. Identification on flood-prone areas by integrated remote sensing model. Lowland Technology International, IALT, **17** (2):105-110.

Iamtrakual. P. and Zhang, J.Y., 2014. Measuring pedestrians, satisfaction of urban environment under transit oriented development (TOD): A case study of Bangkok Metropolitan, Thailand. Lowland Technology International, IALT, **16** (2):125-134.

Peng, F.L., Wang, H.L., Tan, Y., Xu, Z.L. and Li, Y.L., 2011. Field measurements and FEM simulation of a tunnel shaft constructed by pneumatic caisson method in Shanghai soft ground. J. Geotech. and Geoenv. Engrg. ASCE, **137** (5), 516-524.

Qian, S.G., Li, Z.B. and Qiu, Y.S., 2008. Region Classification Report of Geological Hazards in Fuyang. Institute of Geology and Mineral Resources of Zhejiang Province: 1-6 (in Chinese).

Rahmati, A., Faramarzi, L. and Sanei, M., 2014. Development of a new method for RMR and Q classification method to optimize support system in tunneling. Front. Struct. Civ. Engrg., **8** (4): 448-455.

Shahriar K., Sharifzadeh M. and Hamidi J.K., 2008. Geotechnical risk assessment based approach for rock TBM selection in difficult ground conditions. Tunneling and Underground Space Technology, **23** (3): 318-325.

Shen, S.L., Cui, Q.L., Ho, E.C. and Xu, Y.S., 2016. Ground response to multiple parallel Microtunneling operations in cemented silty clay and sand. J. Geotech. and Geoenv. Engrg., **142** (6), 04016001: 1-11.

Shen, S.L., Du, Y.J. and Luo, C.Y., 2010. Evaluation of the effect of double-o-tunnel rolling-correction via apply one-side block loading. Canadian Geotechnical Journal, **47** (10):1060-1070.

Shen, S.L., Wang, J.P., Wu, H.N., Xu, Y.S. and Ye, G.L., 2015b. Evaluation of hydraulic conductivity for both marine and deltaic deposits based on piezocone testing. Ocean Engineering, **110** (2015): 174-182.

Shen, S.L., Wang, Z.F., Yang, J. and Ho, E.C., 2013a. Generalized approach for prediction of jet grout column diameter. J. Geotech. and Geoenv. Engrg., **139** (12), 2060-2069.

Shen, S.L., Wang, Z.F., Horpibulsuk, S, and Kim, Y.H., 2013b. Jet-Grouting with a newly developed technology: the Twin-Jet Method. Engrg. Geol., **152** (1), 87-95.

Shen, S.L., Wu, H.N., Cui, Y.J., Yin, Z.Y., 2014. Long-term settlement behavior of the metro tunnel in Shanghai. Tunneling and Underground Space Technology, **40**: 309-323.

Shen, S.L., Wu, Y.X., Xu, Y.S., Hino, T. and Wu, H.N., 2015a. Evaluation of hydraulic parameters from pumping tests in multi-aquifers with vertical leakage in Tianjin. Computers and Geotechnics, **68** (2015): 196-207.

Shen, S.L., and Xu, Y.S., 2011. Numerical evaluation of land subsidence induced by groundwater pumping in Shanghai. Canadian Geotechnical Journal, **48** (9): 1378-1392.

Shi, J.R., Zhao, X.M., Zheng, F., Hokao, K. and Ge, J., 2013. A quantification analysis of suburb land use and construction intensity based on afar: A case of the land development around Zijingang Campus, Zhejiang University. Lowland Technology International, IALT, **15** (2): 56-65.

Shi, S.S., Li, S.C., Li, L.P., Zhou, Z.Q. and Wang, J., 2014. Advance optimized classification and application of surrounding rock based on fuzzy analytic hierarchy process and tunnel seismic

prediction. Automation in Construction, **37** (2014): 217-222.

Shrestha P.K. and Panthi, K.K., 2014. Groundwater Effect on Faulted Rock Mass: An Evaluation of Modi Khola Pressure Tunnel in the Nepal Himalaya. Rock mechanics and rock engineering, **47** (3): 1021-1035.

Song, J., Miao, L. and Feng, S., 2015. The effect of water boundary conditions of advanced face and lining on the evolution of internal forces in lining. Lowland Technology International, IALT, **17** (1):1-10.

Sowmiya, L.S., Shahu, J.T. and Gupta, K.K., 2015. Performance of geosynthetic reinforcement on the ballasted railway track. Lowland Technology International, IALT, **17** (2): 83-92.

Tan, Y., Li, X., Kang, Z., Liu, J. and Zhu, Y., 2015a. Zoned excavation of an oversized pit close to an existing metro line in stiff clay: case study. J. Perform. Constr. Fac., **29** (6), 04014158: 1-19.

Tan, Y., Wei, B., Zhou, X. and Diao, Y., 2015b. Lessons learned from construction of Shanghai metro stations: importance of quick excavation, prompt propping, timely casting and segmented construction. J. Perform. Constr. Fac., **29** (4), 04014096: 1-15.

Tan, Y., Huang, R., Kang, Z. and Bin, W., 2016. Covered semi-top-down excavation of subway station surrounded by closely spaced buildings in downtown Shanghai: building response. J. Perform. Constr. Fac., 04016040: 1-26.

Tseng, D.J., Tsai, B.R. and Chang L.C., 2011. A case study on ground treatment for a rock tunnel with high groundwater ingression in Taiwan. Tunneling and Underground Space Technology, **16** (3): 175-183.

Wu, F.Q., Miao, J.L., Bao, H. and Wu, J., 2015d. Large deformation of tunnel in slate-schistose rock. Engineering Geology for Society and Territory, **6** (3): 17-23.

Wu, H.G., Wu, D.Y., Ma, H.M. and Zhang, H.L., 2012. Research on type of tunnel-landslide system and tunnel deformation mode. Chinese Journal of Rock Mechanics and Engineering, **31** (supp.2): 3632-3642 (in Chinese).

Wu, H.N., Shen, S.L., Liao, S.M. and Yin, Z.Y., 2015. Longitudinal structural modelling of shield tunnels considering shearing dislocation between segmental rings. Tunneling and Underground Space Technology, **50** (2015): 317-323.

Wu, Y.X., Shen, S.L., Wu, H.N., Xu, Y.S. Yin, Z.Y. and Sun, W.J., 2015a. Environmental protection using dewatering technology in a deep confined aquifer beneath a shallow aquifer. Engrg. Geol., **196** (2015): 59-70.

Wu, Y.X., Shen, S.L., Xu, Y.S. and Yin, Z.Y., 2015b. Characteristics of groundwater seepage with cutoff wall in gravel aquifer. I: Field observations. Canadian Geotechnical Journal, **52** (10): 1526-1538.

Wu, Y.X., Shen, S.L., Yin, Z.Y. and Xu, Y.S., 2015c. Characteristics of groundwater seepage with cutoff wall in gravel aquifer. II: Numerical analysis. Canadian Geotechnical Journal, **52** (10): 1539-1549.

Xiao, Y.Y., Wei, Z., Kazunori H., 2014. Numerical research on building ventilation space in the layouts of residential area. Lowland Technology International, IALT, **16** (2):117-124.

Yao, Q., Chen, H.L., Ye, J.Q., Zhang, W., Li, Q.M. and Liu, J.W., 2008. Direct ESR dating of fault gouge in seismic risk evaluation of southern part of China: exampled with the Fuyang-Yanguan segment of the Xiaoshan-Qiuchuan fault, Hangzhou, China. Bulletin of Science and Technology, **24** (1): 5-9 (in Chinese).

Zarei, H.R., Uromeihy, A. and Sharifzadeh, M., 2011. Evaluation of high local groundwater inflow to a rock tunnel by characterization of geological features. Tunneling and Underground Space Technology, **26** (2011): 364-373.

Zhang, W., Chen, H.L., LI, Q.M., Ding, X.W. and Yao, Q., 2008. The study on Xiaoshao-Qiuchuan faults zone based on remote sensing technique. Bulletin of Science and Technology, **24** (2): 156-161 (in Chinese).

Zhao, Y., Li, P.F. and Tian, S.M., 2013. Prevention and treatment technologies of railway tunnel water inrush and mud gushing in China. J. Rock Mech. and Geotech. Engrg., **5** (2013): 468-477.